IEEE Access
Multidisciplinary Rapid Review Open Access Journal

Received 10 August 2023, accepted 25 August 2023, date of publication 28 August 2023, date of current version 1 September 2023.

Digital Object Identifier 10.1109/ACCESS.2023.3309558

RESEARCH ARTICLE

Primary Distribution Feeder Reinforcement Model With Network Constraints

ABDULLAH A. ALMEHIZIA[1], (Senior Member, IEEE), AND FAHAD S. AL-ISMAIL[2], (Senior Member, IEEE)

[1]Future Energy Institute, King Abdulaziz City for Science and Technology, Riyadh 12354, Saudi Arabia
[2]Department of Electrical Engineering, King Fahad University for Petroleum & Minerals, Dhahran 31261, Saudi Arabia

Corresponding author: Abdullah A. Almehizia (abdullah.almehizia@ieee.org)

ABSTRACT The paper evaluates the primary distribution feeder reinforcement options due to increased electrical demand. A sizing and allocation optimization model based on stochastic Mixed Integer Nonlinear Programming (MINLP) is proposed to realize and asses various electrical distribution feeder upgrade options. The options include transformer reinforcement, adding new cables, installing Photovoltaic (PV) systems, and Battery Energy Storage systems (BESSs). Scenario generation and clustering address the demand and PV power uncertainties. A normal distribution is used to model the demand uncertainty and provide a sensitive insight into the system. The developed model was tested on an 18-bus distribution feeder from an industrial area in Riyadh, Saudi Arabia. The results identified BESS and PV systems as viable reinforcement options.

INDEX TERMS Distribution network expansion, energy storage, feeder upgrade, hybrid systems optimization.

NOMENCLATURE

Subscripts

$BESS$	Battery Energy Storage System.
pv	Photovoltaic.
c	Cables.
tf	Transformer.
g	Electrical grid.

Sets and indices

$\mathbb{I}$	Set of network buses.
$\mathbb{B}_i$	Set of buses connected to bus i.
$\mathbb{T}$	Set of time steps.
$\mathbb{R}$	Set of BESS replacement years.
$\mathbb{Y}$	Set of notations.
$\mathbb{U}$	Set of reduced notations.
$\mathbb{V}$	Set containing all variables.
i, j, k	Network nodes.
n	Year index.
r	Replacement year index.
t	Time step index.
ω	Scenario index.

The associate editor coordinating the review of this manuscript and approving it for publication was Akshay Kumar Saha.

Parameters

$C_y^{o\&m}$	Net present cost of operation and maintenance of element y (\$/unit).
$C_{BESS,P}^{cap}$	Net present cost of capital of the battery's power component (\$/kW).
$C_{BESS,P}^{o\&m}$	Net present cost of operation and maintenance of the battery's power component (\$/kW).
$C_{BESS,E}^{cap}$	Net present cost of capital of the battery's energy component (\$/kWh).
$C_{BESS,E}^{o\&m}$	Net present cost of operation and maintenance of the battery's energy component (\$/kWh).
$C_{BESS,P}^{rep}$	Net present cost of the replacement of the battery's power component (\$/kW).
$C_{BESS,E}^{rep}$	Net present cost of the replacement of the battery's energy component (\$/kWh).
$C_{BESS,P}$	Net present cost of battery power conditioning system (\$/kW).
$C_{BESS,E}$	Net present cost of battery energy (\$/kWh).
$c_y^{o\&m}$	Operation and maintenance cost of element y (\$/unit).
C_{tf}	Net present cost of transformers (\$/kVA).

C_c	Net present cost of cables ($/m).
C_{pv}	Net present cost of photovoltaic systems ($/kW).
C_g	Net present cost of grid supplied energy ($/kWh).
C_{ens}	Net present cost of energy not served ($/kWh).
β, γ	Interest and inflation rates respectively (%).
N_p	Project lifetime (Years).
r_{ij}, x_{ij}	Resistance and reactance between buses i and j respectively.
$S_{tf,ij}, S_{c,ij}$	Complex power capacity transformers and cables between buses i and j respectively (kVA).
$S_{L,i,t}, \mathrm{pf}_{L,i,t}$	Complex power demand and power factor at bus i in time t respectively (kVA).
$P^{\omega}_{L,i,t}, Q^{\omega}_{L,i,t}$	Real and reactive power demand at bus i in time t in scenario ω respectively (kW).
Δt	Time step (Hour).
n_{tf}, n_c	Lifetime of newly installed transformers and cables respectively (Years).
n_{BESS}	Lifetime of newly installed batteries (Years).
$\eta^{ch}_{bat}, \eta^{dis}_{bat}$	Battery efficiency for charging and discharging respectively (%).
Ω	Number of scenarios.
$p^{\omega}_{pv,t}$	Power output of 1kW PV in time t in scenario ω (kW).

Variables

$P^R_{BESS,i}$	Battery's rated power at bus i (kW).
$E^R_{BESS,i}$	Battery's rated energy at bus i (kWh).
P^R_{pv}	Solar PV rated power capacity (kW).
$P^{\omega}_{pv,t}$	Power output of the solar PV system in time t in scenario ω (kW).
$\delta_{tf,ij}$	Additional transformer capacity installed between buses i and j (kVA).
$\delta_{c,ij}$	Additional cables installed between buses i and j (Unit).
$\Phi_{tf,ij}$	Equivalent circuit multiplier for transformers.
$\Phi_{c,ij}$	Equivalent circuit multiplier for cables.
P_{pv}	PV plant capacity (kW).
E^{ω}_G	Energy supplied from the grid in scenario ω (kWh).
ENS^{ω}	Energy not served in scenario ω (kWh).
$P^{\omega}_{ij,t}, Q^{\omega}_{ij,t}$	Real and reactive power flow form bus i to j at time t in scenario ω respectively (kW).
$P^{\omega}_{BESS,i,t}$	Charging/ discharging battery power at bus i in time t in scenario ω (kW).
$P^{\omega}_{G,i,t}, Q^{\omega}_{G,i,t}$	Real and reactive power injected at bus i in time t in scenario ω respectively (kW).
$V^{\omega}_{i,t}, V^{\omega}_{j,t}$	Voltage magnitudes at buses i and j at time t in scenario ω respectively (V).
$P^{\omega}_{dis,i,t}$	Battery real power discharge at bus i in time t in scenario ω (kW).
$P^{\omega}_{ch,i,t}$	Battery real power charge at bus i in time t in scenario ω (kW).
$u^{\omega}_{1,i,t}, u^{\omega}_{2,i,t}$	Binary variable for the battery real and reactive power charging status (0,1) respectively in scenario ω.
$u^{\omega}_{3,i,t}$	Binary variable for the load shedding status (0,1) in scenario ω.
$E^{\omega}_{BESS,i,t}$	Battery storage capacity at bus i in time t in scenario ω (kWh).
$E^{\min}_{BESS,i,t}$	Minimum battery state of charge at bus i (kWh).

I. INTRODUCTION

A. DISTRIBUTION NETWORK AND FEEDER DEFINITION

The electric power distribution is a fundamental part of the value chain of the electrical power industry. Responsible for delivering electrical energy from high-voltage transmission systems to the end users. Typically the distribution system comprises two segments, primary and secondary distribution [1].

The primary distribution system is a medium-voltage network (4)-69 kV), where the substation transformers step down the voltage from the transmission to distribution levels. The electrical energy is carried out from the substation through a three-phase distribution feeder with a capacity limit defined in (MVA), which usually connects substations to distribution transformers for further voltage step-down (207-400 V) line-to-line values. The secondary distribution network distributes energy at the customers' utilization voltages from the distribution transformers downward [2].

The distribution networks are capital-intensive businesses [3], and distribution expansion planning (DEP) is required to attain low cost and high reliability for electrical energy delivery. Different aspects are involved in a distribution planning study, including technical, economic, regulatory, and environmental aspects.

B. MOTIVATION AND PROBLEM DESCRIPTION

A typical DEP's goal is to locate and size distribution substations, distributed generators (DGs), and distribution feeders best to fulfill future needs in a timely and cost-effective way while meeting all limitations and technical standards [4]. The evolution of modern distribution networks requires attention to newer solutions, including renewable energy and storage systems. Deploying battery energy storage systems (BESSs) and renewable energy resources, namely PVs, can maximize a distribution network's energy efficiency. Optimally placing BESS can handle peak energy demand, mitigate network losses, relieve the technical challenges of integrating renewables, manage power quality issues, and reduce expansion costs [5].

C. RELATED WORK

Many studies regarding DEP are reported in the literature. A comprehensive distribution network expansion planning

(DNEP) review is reported in [6]. The review examined the various modeling schemes related to such planning problems. These include objective functions, constraints, time horizons, and uncertainties. The level of complexity in distribution networks is the major DNEP problem. Different constraints must be handled, including power balancing, level of voltages, the power capacity of the feeders, DG limitations, radiality constraints, and emissions. The study concluded with several findings. The first conclusion is that mathematical methods were more accurate than Artificial Intelligence (AI) techniques. The second conclusion states that Genetic Algorithms (GA) were extensively utilized to solve the problem in the reported literature. The third conclusion suggests hybrid methods are suitable for reducing computational time in searching for optimum solutions in a comparatively short duration. The fourth conclusion incites that the objectives of such planning problems are a trade-off between the accuracy of solutions provided, reliability, and the time required for solving the problem. Finally, expansion planning that is more economical and reliable can be achieved with the integration of DGs.

The authors of [7] proposed an expansion planning model for a radial distribution network with DGs. The objective is to minimize the cost of investment, losses, customer interruptions and lost DG production. The decision variables are taken as the complete feeder, consisting of cables and transformers as a single unit of the upgrade, with a cost per unit associated. The solution of the model was carried out using mixed integer linear programming (MILP) and heuristic methods, namely simulated annealing (SA). The model developed did not include energy storage as a potential candidate for upgrading the network. In addition, the limitation of line capacity is calculated with a simplistic model in the power balance constraint.

In the paper [8], a simple model to assess the benefit of energy storage to defer upgrades on a distribution feeder was proposed. The model considered different load growth rates as the sensitivity for assessment. The model included the feeder and BESS as the variables of the problem. Empirical data was used to identify the cost of the power and energy components of the BESS. A benefits evaluation metric was designed to determine the deferral benefits as a function of deferral duration and load growth rate. However, The model lacked an optimization model and network technical constraints. Another similar attempt for assessing energy storage for upgrade deferral was reported in [9]. A sample of feeders was selected to evaluate the viability of energy storage to defer upgrades. Peak shaving and reactive power compensation were investigated as applications of energy storage. Only BESSs were considered as an option for upgrade deferral. The technical study was performed utilizing CYME software, where power flow studies were conducted, considering real and reactive power flows in the network. The developed model did not investigate the possibility of feeder and transformer upgrades. Furthermore, optimized sizing and location of the energy storage were not part of the study.

In [10], the authors presented the benefits provided by BESSs in the electrical network and different technologies of BESS. The paper's primary purpose was to investigate BESS's viability in upgrading the capacity of substations. It was concluded that electrical components of the distribution network could be handled under their limits using BESS, increasing the power control's flexibility. The paper lacked a BESS optimization model for size and location.

Reference [11], evaluated the techno-economic benefits of BESSs in the distribution network. They presented a model for network upgrade deferral as a function of renewable penetration, load growth, and the fraction of load shaving. The optimization problem considers the feeder, transformers, and BESS as decision variables. The model adopted DC power flow to handle real power limitations, which raised an issue of not accounting for the reactive power in the network. Also, the sizing for renewable is done in a simplistic step-wise matter without optimization.

D. CONTRIBUTIONS

The proposed paper developed an optimization model to account for various feeder upgrade options, including line reinforcement, transformer capacity upgrade, PV systems, and BESSs installation at the distribution level, accounting for both active and reactive power capabilities. A stochastic model is formed and solved where samples represent numerous scenarios of the uncertain parameter from their associated probability distribution.

The contributions of the proposed paper are summarized in the following:

1) Provide a detailed planning and operation model to assess the contribution of various reinforcement actions.
2) Accounting for the impact of topology reconfiguration based on adding new cables and transformers.

The solution of the proposed model would provide the location and capacity of the considered upgrade equipment to meet the increase in demand at the lowest cost possible.

E. PAPER ORGANIZATION

The organization of the paper is as follows. Section II defines the system adopted in the paper. Section III derives the mathematical formulation. Section IV demonstrates the uncertainty modeling utilized. Numerical simulations, results, and discussion are presented in Section V. Section VI concludes the paper with insights and remarks.

II. SYSTEM COMPONENTS

The reinforcement components include installing PV systems, BESS, and upgrading cables and transformers. Incorporating Electric vehicles (EVs), wind turbines, and hydrogen storage are not in the scope of the paper.

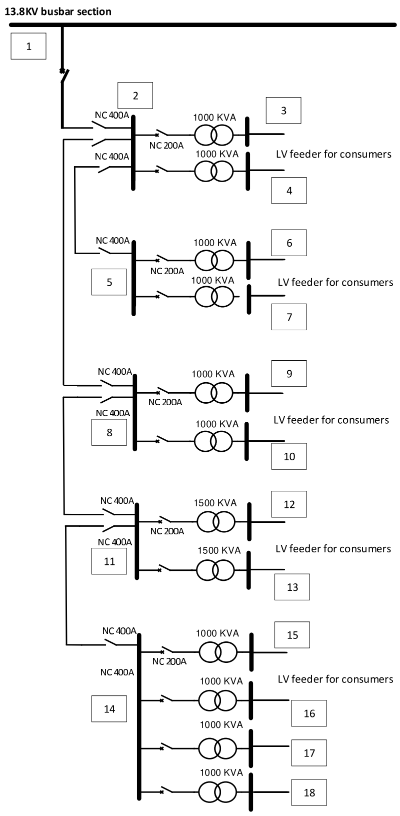

FIGURE 1. 18 bus distribution feeder.

A. SUBSTATION MODEL

The electrical grid energy (E_G^{ω}) is supplied through a substation from which various primary distribution feeders deliver the power through the various distribution transformers. In figure 1, bus one represents the slack bus of the network [12], [13].

B. DISTRIBUTION FEEDER MODEL

The distribution network typically has two main elements: distribution transformers and cables. It is essential to identify their impedances (r_{ij}, x_{ij}) for modeling these two components. Figure 1 depicts the primary distribution feeder. It shows a radial industrial distribution feeder (13.8 kV) supplying twelve distribution transformers (13.8/0.4 kV), feeding factories, in the Riyadh region, Saudi Arabia [14], [15].

C. PV SYSTEM MODEL

The PV system is centralized and connected to the main feeder's bus (bus 1) through the medium-voltage transformer at the substation. The System Advisor Model (SAM) [16] calculates the hourly power output ($p_{pv,t}^{\omega}$) for the entire year.

D. BESS MODEL

This paper assumes lithium-ion batteries to be installed. with a fixed charging/discharging efficiency (η_{bat}) of 95% [17], [18].

E. LOAD MODEL

Each transformer load demand ($P_{L,i,t}^{\omega}, Q_{L,i,t}^{\omega}$) assumes an hourly time series of constant power values. The raw data was collected by transformer meters.

III. MATHEMATICAL FORMULATION

A. COST MODEL

The cost models for the system components are adopted from [19]:

$$C_y^{o\&m} = c_y^{o\&m} \sum_{n=1}^{N_p} \left(\frac{1+f}{1+i}\right)^n \tag{1}$$

$$C_{BESS}^{rep} = c_{BESS}^{rep} \sum_{r \in \mathbb{R}} \left(\frac{1+f}{1+i}\right)^r \tag{2}$$

$$C_u = C_u^{cap} + C_u^{o\&m} \tag{3}$$

$$\begin{aligned} C_{BESS} &= C_{BESS}^{cap} + C_{BESS}^{o\&m} + C_{BESS}^{rep} \\ \mathbb{Y} &= \{BESS, c, pv\}, \quad \mathbb{U} = \{c, pv\} \end{aligned} \tag{4}$$

Equation (1) is the net present cost of each system component's operation and maintenance cost denoted by y. The net present cost of the replacement is considered for the energy storage and calculated by equation (2). The total net present cost for the cables and PVs is calculated using equation (3). The total net present cost for the energy storage is calculated by equation (4). The total cost of ownership model reported in [20] was used to model the distribution transformers' cost.

B. OBJECTIVE FUNCTION

The optimization formulation is related to minimizing the system cost, including installing the PV system, adding cables, transformers, and BESS, in addition to the operation cost represented by the energy supplied from the grid and the cost of unserved demand as in (5).

$$\begin{aligned} \min_{\substack{P_{pv}^R, P_{BESS,i}^R, E_{BESS,i}^R, \\ \delta_{tf,ij}, \delta_{c,ij}, \\ E_g^{\omega}, \mathrm{ENS}^{\omega}}} \quad & C_{pv} P_{pv}^R + \sum_{i \in \mathbb{I}} C_{BESS,P} P_{BESS,i}^R \\ & + \sum_{i \in \mathbb{I}} C_{BESS,E} E_{BESS,i}^R \\ & + \sum_{i \in \mathbb{I}} \sum_{j \in \mathbb{B}_i} C_{tf} \delta_{tf,ij} + \sum_{i \in \mathbb{I}} \sum_{j \in \mathbb{B}_i} C_c \delta_{c,ij} + \frac{365}{\Omega} \sum_{\omega=1}^{\Omega} C_g E_G^{\omega} \\ & + \frac{365}{\Omega} \sum_{\omega=1}^{\Omega} C_{ens} \mathrm{ENS}^{\omega} \end{aligned} \tag{5}$$

C. POWER BALANCE CONSTRAINTS

The paper adopts a linearized DistFlow model [15], [21], [22], [23] for power flow calculations

$$\begin{aligned} \sum_{j \in \mathbb{B}_i} P_{ij,t}^{\omega} - \sum_{k \in \mathbb{B}_i} P_{ki,t}^{\omega} &= P_{G,t}^{\omega} + P_{pv,t}^{\omega} + P_{BESS,i,t}^{\omega} \\ & \quad - (1 - u_{3,i,t}^{\omega}) P_{L,i,t}^{\omega}, \quad \forall i, \forall t, \forall \omega \end{aligned} \tag{6}$$

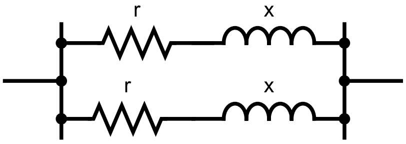

FIGURE 2. Two line network

$$\sum_{j\in\mathbb{B}_i} Q^{\omega}_{ij,t} + \sum_{k\in\mathbb{B}_i} Q^{\omega}_{ki,t} = Q^{\omega}_{G,t} + Q^{\omega}_{BESS,i,t} - (1 - u^{\omega}_{3,i,t})Q^{\omega}_{L,i,t}, \quad \forall i, \forall t, \forall \omega \tag{7}$$

$$\mathrm{ENS}^{\omega} = \sum_{i\in\mathbb{I}} \sum_{t\in\mathbb{T}} u^{\omega}_{3,i,t} P^{\omega}_{L,i,t}, \qquad \forall \omega \tag{8}$$

$$E^{\omega}_{g} = \sum_{t\in\mathbb{T}} P^{\omega}_{G,t}, \qquad \forall \omega \tag{9}$$

$$P^{\omega}_{pv,t} \leq P^{R}_{pv} p^{\omega}_{pv,t}, \qquad \forall t, \forall \omega \tag{10}$$

$$P^{\omega}_{pv,t} \geq 0, \qquad \forall t, \forall \omega \tag{11}$$

Constraints (6) and (7) represent the load balancing constraint stating that for any time instant t in realization ω, the supply must be sufficient to the required demand for active and reactive powers. Constraints (8) and (9) define the energy not served and the energy supplied by the electrical grid to the network, respectively. The PV power output is constrained by (10) and (11).

D. NETWORK CONFIGURATION CONSTRAINTS

Adding new elements to the network, such as distribution transformers and cables, would change the equivalent impedance. As such, the optimization model should be adaptive to the change of the impedances of the network for accurate representation and results. Therefore, two variables are defined to account for the change in network impedance. The derivation of these variables $\Phi_{c,ij}$ and $\Phi_{tf,ij}$ are deduced from basic circuit theory [2].

Figure 2 represents a simple cable model with series resistance and reactance, and the series impedance Z is given by:

$$Z = r_{ij} + jx_{ij} \tag{12}$$

For a two-parallel line network, the equivalent circuit impedance Z_{eq} is:

$$Z_{eq} = \frac{Z.Z}{Z+Z} = \frac{Z^2}{2Z} = \frac{Z}{2} \tag{13}$$

And for a three-parallel line network:

$$Z_{eq} = \frac{Z/2.Z}{Z/2+Z} = \frac{Z^2}{3Z} = \frac{Z}{3} \tag{14}$$

A generalization can easily be formed for any number of additional parallel lines:

$$Z_{eq} = \frac{1}{1+\delta_{c,ij}} Z \tag{15}$$

Notice when no additional lines are added ($\delta_{c,ij} = 0$), equation (15) reduces to $Z_{eq} = Z$.

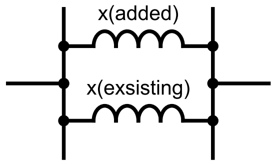

FIGURE 3. Paralleling model of two transformers

As for the transformers, the reactance model shown in figure 3 is used for simplicity. The percentage impedance of two transformers connected in parallel should be the same for load sharing based on the transformer capacity. Since the problem is represented in a per-unit system, any added transformer impedance must be converted to the per-unit value of the MVA base used in the problem. The conversion equation is as follows:

$$x'_{pu} = x_{pu,added} \left(\frac{\mathrm{kV}_{added}}{\mathrm{kV}_{base}}\right)^2 \left(\frac{\mathrm{MVA}_{base}}{\mathrm{MVA}_{added}}\right) \tag{16}$$

where x'_{pu} is the reactance of the added transformer converted to the MVA base of the problem. $x_{pu,added}$ is the reactance of the added transformer in per unit. Since the voltage levels would not change ($\mathrm{kV}_{base} = \mathrm{kV}_{added}$) equation (16) reduce to:

$$x'_{pu} = x_{pu,added} \left(\frac{\mathrm{MVA}_{base}}{\mathrm{MVA}_{added}}\right) \tag{17}$$

$$\delta_{tf,ij} = \left(\frac{\mathrm{MVA}_{added}}{\mathrm{MVA}_{base}}\right) \tag{18}$$

$$x'_{pu} = \frac{1}{\delta_{tf,ij}} x_{pu,added} \tag{19}$$

As previously mentioned, the percentage impedance of two paralleled transformers are equal $x_{pu,added} = x$

Dropping the (pu) notation, the equivalent reactance of the transformers connected in parallel x_{eq} is calculated.

$$x_{eq} = \frac{x.x'}{x+x'} = \frac{x\frac{x}{\delta_{tf,ij}}}{x+\frac{x}{\delta_{tf,ij}}} = \frac{1}{1+\delta_{tf,ij}} x \tag{20}$$

where x is the per unit impedance of the existing transformer. Notice as well when no additional transformer is connected ($\mathrm{MVA}_{added} = 0$) equation (20) reduces to $x_{eq} = x$

We are now ready to write the multipliers required for calculating network impedances as they change depending on the cables and transformers added to the network. The following constraints are added to account for the equivalent network model and will be used to calculate the voltage drop between the buses shown in subsection H.

$$\Phi_{c,ij} = \frac{1}{1+\delta_{c,ij}}, \tag{21}$$

$$\Phi_{tf,ij} = \frac{1}{1+\delta_{tf,ij}} \tag{22}$$

The constraints (21) and (22) are for calculating the equivalent circuit model subjected to adding new cables or transformers.

E. LINE FLOW CONSTRAINTS

The power flow through the cables should not exceed its capacity. As such, the following constraints are implemented [24], [25], [26].

$$-(1+\delta_{c,ij})S_{c,ij} \leq P^{\omega}_{ij,t} \leq (1+\delta_{c,ij})S_{c,ij}, \quad \forall t, \forall \omega \quad (23)$$

$$-(1+\delta_{c,ij})S_{c,ij} \leq Q^{\omega}_{ij,t} \leq (1+\delta_{c,ij})S_{c,ij}, \quad \forall t, \forall \omega \quad (24)$$

$$-\sqrt{2}(1+\delta_{c,ij})S_{c,ij} \leq P^{\omega}_{ij,t} + Q^{\omega}_{ij,t} \leq \sqrt{2}(1+\delta_{c,ij})S_{c,ij}, \quad \forall t, \forall \omega \quad (25)$$

$$-\sqrt{2}(1+\delta_{c,ij})S_{c,ij} \leq P^{\omega}_{ij,t} - Q^{\omega}_{ij,t} \leq \sqrt{2}(1+\delta_{c,ij})S_{c,ij}, \quad \forall t, \forall \omega \quad (26)$$

The inequalities (23) to (26) are the line flow constraints, which ensure the loading of the cables does not exceed the total capacity of the line for all time instances t in all realizations of ω.

F. TRANSFORMER FLOW CONSTRAINTS

Similar to the line flow constraints, the power flow through the transformers should not exceed its capacity. As such, the following constraints are implemented [24], [25], [26].

$$-(1+\delta_{tf,ij})S_{tf,ij} \leq P^{\omega}_{ij,t} \leq (1+\delta_{tf,ij})S_{tf,ij}, \quad \forall t, \forall \omega \quad (27)$$

$$-(1+\delta_{tf,ij})S_{tf,ij} \leq Q^{\omega}_{ij,t} \leq (1+\delta_{tf,ij})S_{tf,ij}, \quad \forall t, \forall \omega \quad (28)$$

$$-\sqrt{2}(1+\delta_{tf,ij})S_{tf,ij} \leq P^{\omega}_{ij,t} + Q^{\omega}_{ij,t} \leq \sqrt{2}(1+\delta_{tf,ij})S_{tf,ij}, \quad \forall t, \forall \omega \quad (29)$$

$$-\sqrt{2}(1+\delta_{tf,ij})S_{tf,ij} \leq P^{\omega}_{ij,t} - Q^{\omega}_{ij,t} \leq \sqrt{2}(1+\delta_{tf,ij})S_{tf,ij}, \quad \forall t, \forall \omega \quad (30)$$

The inequalities (27) to (30) are the transformer flow constraints, which ensure the loading on the transformers does not exceed the total capacity for all time instances t in all realizations of ω.

G. BATTERY ENERGY STORAGE SYSTEM CONSTRAINTS

The operation of the BESS is subjected to the following constraints [27].

$$0 \leq P^{\omega}_{dis,i,t} \leq S^{R}_{BESS,i} u_{1,i,t}, \quad \forall t, \forall \omega \quad (31)$$

$$-S^{R}_{BESS,i}(1-u^{\omega}_{1,i,t}) \leq P^{\omega}_{ch,i,t} \leq 0, \quad \forall t, \forall \omega \quad (32)$$

$$0 \leq Q^{\omega}_{dis,i,t} \leq S^{R}_{BESS,i} u_{2,i,t}, \quad \forall t, \forall \omega \quad (33)$$

$$-S^{R}_{BESS,i}(1-u^{\omega}_{2,i,t}) \leq Q^{\omega}_{ch,i,t} \leq 0, \quad \forall t, \forall \omega \quad (34)$$

$$P^{\omega}_{BESS,i,t} = P^{\omega}_{dis,i,t} + P^{\omega}_{ch,i,t}, \quad \forall t, \forall \omega \quad (35)$$

$$Q^{\omega}_{BESS,i,t} = Q^{\omega}_{dis,i,t} + Q^{\omega}_{ch,i,t}, \quad \forall t, \forall \omega \quad (36)$$

$$-\sqrt{2}S^{R}_{BESS,i} \leq P^{\omega}_{BESS,i,t} + Q^{\omega}_{BESS,i,t} \leq \sqrt{2}S^{R}_{BESS,i}, \forall t, \forall \omega \quad (37)$$

$$-\sqrt{2}S^{R}_{BESS,i} \leq P^{\omega}_{BBESS,i,t} - Q^{\omega}_{ESS,i,t} \leq \sqrt{2}S^{R}_{BESS,i}, \forall t, \forall \omega \quad (38)$$

$$E^{\omega}_{BESS,i,t+1} = E^{\omega}_{BESS,i,t} - \left(\frac{P^{\omega}_{dis,i,t}}{\eta_{dis}} - \eta_{ch}P^{\omega}_{ch,i,t}\right)\Delta t, \forall t, \forall \omega \quad (39)$$

$$E^{\min}_{BESS,i} \leq E^{\omega}_{BESS,i,t} \leq E^{R}_{BESS,i}, \quad \forall t, \forall \omega \quad (40)$$

$$E^{\min}_{BESS,i} = 0.2\, E^{R}_{BESS,i} \quad (41)$$

The constraints (31) to (34) limits the batteries' charging and discharging of active and reactive power within its total capacity. Constraint (35) and (36) is to define a variable for the active and reactive power supplied or consumed by the batteries. The total complex power supplied by the batteries is restricted by constraints (37) and (38). Constraint (39) defines the state of charge in the BESS at all instances. Constraint (40) states that the stored energy shall not exceed the batteries' capacity and should not reach the minimum charge state. Constraint (41) sets the minimum state of charge for each BESS. All the constraints should be imposed for all instances t in all realizations of ω.

H. VOLTAGE LEVEL CONSTRAINTS

The voltage level at every bus in the network is crucial for the safe operation of the network and should be within the normal operating range. Network constraints (21) and (22) are utilized here to account for the changes in the equivalent circuit. The following constraints give the calculation of the voltage drop [21], [22], [23].

$$|V^{\omega}_{i,t}|^2 - |V^{\omega}_{j,t}|^2 = 2(r_{ij}\Phi_{c,ij}P^{\omega}_{ij,t} + x_{ij}\Phi_{c,ij}Q^{\omega}_{ij,t}), \quad \forall t, \forall \omega \quad (42)$$

$$|V^{\omega}_{i,t}|^2 - |V^{\omega}_{j,t}|^2 = 2(x_{ij}\Phi_{tf,ij}Q^{\omega}_{ij,t}), \quad \forall t, \forall \omega \quad (43)$$

$$V^{\min}_{i} \leq V^{\omega}_{i,t} \leq V^{\max}_{i}, \quad \forall t, \forall \omega \quad (44)$$

The constraint (42) is for calculating the voltage drop between two buses of a cable. Constraint (43) is for calculating the voltage drop between two buses of a transformer. The voltage level is constrained by (44) to be within an acceptable operating range. All the constraints should be imposed for all instances of t in all realizations of ω.

I. OPTIMIZATION PROBLEM FORMULATION

This subsection is meant to summarize and clearly describe the optimization problem formulated. *Objective function*: Minimizing system planning and operation cost

align (5)
Constraints:
Power Balance
Equations (6) to (9)
PV Power
Equations (10) to (11)
Network Configuration
Equations (21) and (22)
Line Flow
Equations (23) to (26)
Transformer Flow

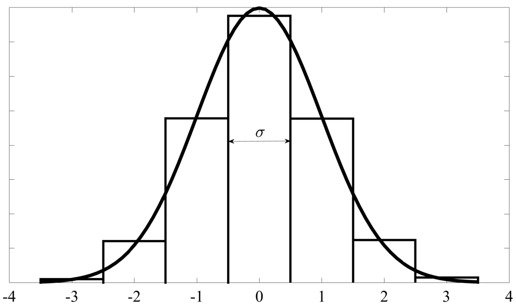

FIGURE 4. Discretization of the probability distribution of the load demand.

Equations (27) to (30)
Battery Energy Storage System
Equations (31) to (41)
Voltage Level
Equations (42) and (44)
Variable bounds
$\mathbb{V} \geq 0$

IV. UNCERTAINTY MODELING

The main sources of uncertainty in the proposed problem are the load demand and the power output of the solar PV system. This paper relies on previous research for handling the uncertainty [28], [29], [30] and does not claim novelty as it is out of the scope of the paper.

A. LOAD DEMAND

A normal distribution is usually used to model the uncertainty of the demand. For a realistic description, each demand bus of the feeder is represented by a normal distribution with a unique mean value and standard deviation, making each bus unique from other buses. Figure 4 shows a typical normal probability distribution. The normal distribution of the load demand is used to generate a large number of scenarios (10000 scenarios). Then k-means clustering algorithm is utilized to reduce the number of scenarios for the problem to be tractable, as shown in algorithm 2.

B. PV POWER

As for the solar power uncertainty, hourly data of a typical 1kW panel $p_{pv,t}$ power output was collected and arranged for each month. Then divided into four periods; each period comprises three months. An average hourly value is calculated for each period resulting in 96 data points and each 24 data points is considered a scenario as shown in algorithm 3.

V. NUMERICAL RESULTS

A. SYSTEM DATA AND PARAMETERS

The General Algebraic Modeling System (GAMS) was utilized to model and solve the optimization problem. SCIP solver was used for solving the model. The data shown in Table 2 were compiled from various references, including the Saudi Electricity Company (SEC), and references [31] and [32]. The operational model duration is (T=96 hours), representing four days, and each day is considered a scenario. Figure 5 shows a flowchart of the complete simulation model.

Algorithm 1 Demand Scaling

Input: $(\mathbb{I}, \mathbb{T}, S_{L,i,t}, \mathrm{pf}_{L,i,t}, p = 100\%, 120\%, 140\%, 160\%)$
Output: $P_{L,i,t}, Q_{L,i,t}$

for $i \in \mathbb{I}$
  $S^{\max}_{L,i} = \max(S_{L,i,t}) \rightarrow df_{L,i} = S_{tf,ki}/S^{\max}_{L,i}$
  $S^{100\%}_{L,i,t} = df_{L,i}S_{L,i,t},\ S^{120\%}_{L,i,t} = 1.2S^{100\%}_{L,i,t}$
  $S^{140\%}_{L,i,t} = 1.4S^{100\%}_{L,i,t},\ S^{160\%}_{L,i,t} = 1.6S^{100\%}_{L,i,t}$
  $P^{p}_{L,i,t} = S^{p}_{L,i,t}pf_{L,i,t}$
  $Q^{p}_{L,i,t} = (S^{p}_{L,i,t})^2 - (P^{p}_{L,i,t})^2$
end

Algorithm 2 Demand Uncertainty

Input: $(\mathbb{I}, \mathbb{T}, P_{L,i,t}, Q_{L,i,t}, s = 10000, \Omega = 4)$
Output: $P^{\omega}_{L,i,t}, Q^{\omega}_{L,i,t}, \quad \omega = 1, \ldots \Omega$

for $i \in \mathbb{I}$
  for $t \in \mathbb{T}$
    $\mu, \sigma \leftarrow$ Extract(mean *and* standard deviation) from $P_{L,i,t}, Q_{L,i,t}$
    $\mathcal{P} \leftarrow N \sim (\mu, \sigma)$ Generate probability distribution functions
    $\tilde{\omega} \leftarrow$ Sample ($\mathcal{P}$ and make s number of scenarios)
    $\omega \leftarrow$ Perform k-means clustering to reduce scenarios to Ω clusters
  end
end

Algorithm 3 PV Power Uncertainty

Input: $(\mathbb{T}, p_{pv,t})$
Output: $p^{\omega}_{pv,t}, \quad \omega = 1, \ldots, \Omega$

$p_{pv,m} \leftarrow$ Divied($p_{pv,t}$) into monthly matrices
for $m = 1 : 12$
  $p_{pv,avg,m} \leftarrow$ Mean($p_{pv,m}$) calculate monthly mean
end
$p^{\omega=1}_{pv,t} \leftarrow \mathrm{Mean}(p_{pa,avg,1} + p_{pa,avg,2} + p_{pa,avg,3})$
$p^{\omega=2}_{pv,t} \leftarrow \mathrm{Mean}(p_{pa,avg,4} + p_{pa,avg,5} + p_{pa,avg,6})$
$p^{\omega=3}_{pv,t} \leftarrow \mathrm{Mean}(p_{pa,avg,7} + p_{pa,avg,8} + p_{pa,avg,9})$
$p^{\omega=4}_{pv,t} \leftarrow \mathrm{Mean}(p_{pa,avg,10} + p_{pa,avg,11} + p_{pa,avg,12})$

B. SIMULATION RESULTS

1) CASE A: DISTRIBUTION FEEDER UPGRADE (RETROFITTING)

To test the developed model for network upgrade, the expected load demand for each transformer is scaled from its original values. This is done since the measured demand was significantly below the capacity of the distribution transformers. To consider any upgrade options for the feeder, the demand should exceed the current limitations of the equipment. Thus, the scaling algorithm (Algorithm 1) was adopted. The data of the feeder is shown in Table 1.

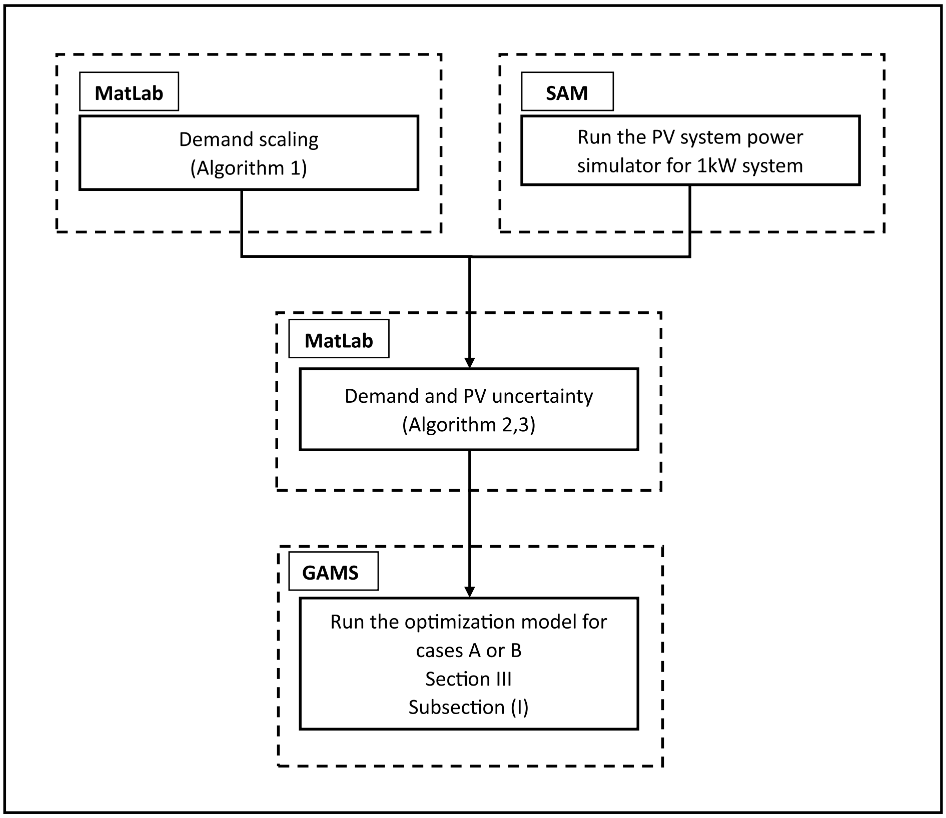

FIGURE 5. flowchart of the developed model.

TABLE 1. Feeder components and capacities.

Bus	Electrical Apparatus	Capacity (kVA)
2-3	Transformer	1000
2-4	Transformer	1000
5-6	Transformer	1000
5-7	Transformer	1000
8-9	Transformer	1000
8-10	Transformer	1000
11-12	Transformer	1500
11-13	Transformer	1500
14-15	Transformer	1000
14-16	Transformer	1000
14-17	Transformer	1000
14-18	Transformer	1000
1-2	Cable	9000
2-5	Cable	9000
2-8	Cable	9000
8-11	Cable	9000
11-14	Cable	9000

TABLE 2. System economic parameters.

Parameters	Values
i, f (%)	2.7, 2.3
N_P, n_{BESS} (Years)	25, 10
$c^{cap}_{BESS,P}$ (\$/kW)	230
$c^{cap}_{BESS,E}$ (\$/kWh)	240
c^{cap}_{tf} (\$/kVA)	511
c^{cap}_{c} (\$/m)	88
c^{cap}_{pv} (\$/kW)	1040
$c^{o\&m}_{BESS,P}$ (\$/kW-yr)	0.025 $c^{cap}_{BESS,P}$
$c^{o\&m}_{BESS,E}$ (\$/kWh-yr)	0.025 $c^{cap}_{BESS,E}$
$c^{o\&m}_{pv}$ (\$/kW-yr)	13
$c^{rep}_{BESS,P}$ (\$/kW)	0.5 $c^{cap}_{BESS,P}$
$c^{rep}_{BESS,E}$ (\$/kWh)	0.5 $c^{cap}_{BESS,E}$

Case A represented an existing feeder to be reinforced. The reinforcement solution involved adding cables, transformers, BESSs, and a PV system for a load scaled by 120%, 140%, and 160% of transformer capacity. The expansion plan is shown in Table 3, and Table 4 shows BESS capacity and location.

Table 3 demonstrates a trend of increased capacity for the transformers as the load increases. A similar trend can be observed for the PV capacity as well. As a result, the system's total cost also increased, as shown in Table 5.

The main cable (Cable 1-2) is reinforced with an additional line for all cases. The reason is this line carries all the energy in the feeder as it distributes power radially.

An interesting situation for case 120% is at buses 3 (transformer 2-3), 10 (transformer 8-10), and 12 (transformer 11-12) for cases 120% and 140%. No expansion for the transformers was involved, as shown in Table 3. However, a BESS was installed instead to cope with the increased demand, as seen in Table 4.

TABLE 3. Network upgrades of test case A.

Bus	Electrical Apparatus	Expansion Capacity (KVA)		
		120%	140%	160%
2-3	Transformer	-	113	358
2-4	Transformer	60	209	337
5-6	Transformer	306	467	750
5-7	Transformer	89	213	466
8-9	Transformer	76	303	476
8-10	Transformer	-	-	48
11-12	Transformer	-	-	101
11-13	Transformer	400	692	1014
14-15	Transformer	204	338	532
14-16	Transformer	312	414	697
14-17	Transformer	351	749	944
14-18	Transformer	52	204	366
1-2	Cable	1 (unit)	1 (unit)	1 (unit)
2-5	Cable	-	-	-
2-8	Cable	-	1 (unit)	1 (unit)
8-11	Cable	-	-	1 (unit)
11-14	Cable	-	-	-
1	PV	16057 (kW)	20100 (kW)	22857 (kW)

TABLE 4. Battery energy storage system for load demand of test case A.

Bus	120%		140%		160%	
	Power (kVA)	Energy (kWh)	Power (kVA)	Energy (kWh)	Power (kVA)	Energy (kWh)
1	-	-	-	-	-	-
2	-	-	-	-	-	-
3	236	224	394	415	375	381
4	316	300	387	553	472	448
5	-	-	-	-	-	-
6	114	108	155	224	95	91
7	106	223	285	328	251	269
8	-	-	-	-	-	-
9	224	213	212	333	327	310
10	432	1104	670	1549	828	2087
11	-	-	-	-	-	-
12	386	531	704	1657	972	2728
13	258	737	319	569	343	541
14	-	-	-	-	-	-
15	121	163	290	464	287	353
16	30	85	186	352	226	318
17	188	256	-	-	76	80
18	264	527	392	788	439	511

The figures 6 to 10 below show the operation of the active power of the BESS for the situations where transformer upgrades were not involved. Including transformer (2)-(3) for case 120%, and transformers (8)-(10) and (11)-(12) for cases 120% and 140%. Charging operation is represented as a negative power, and discharging as a positive power. As a general observation for all cases, the charging period coincides with the availability of PV power, as shown in figure 17.

It can be observed that the demand has exceeded the capacity of the transformers (marked in red), and the BESS has supplied the deficit in active power. Furthermore, a reverse power flow has occurred several times (marked in black), indicating that the BESS is supplying other loads in addition to its connected one.

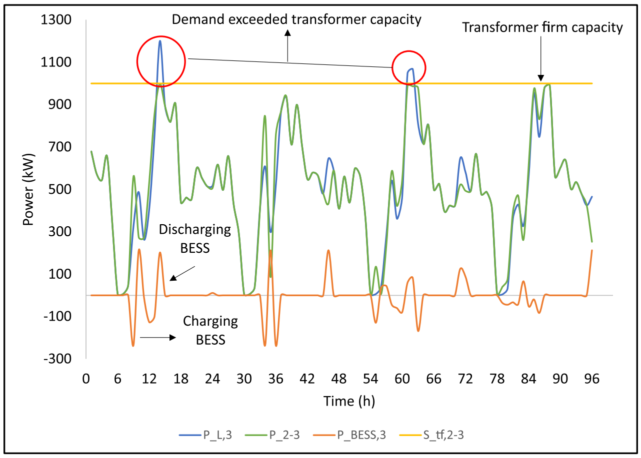

FIGURE 6. Battery active power operation at bus 3 for case 120%.

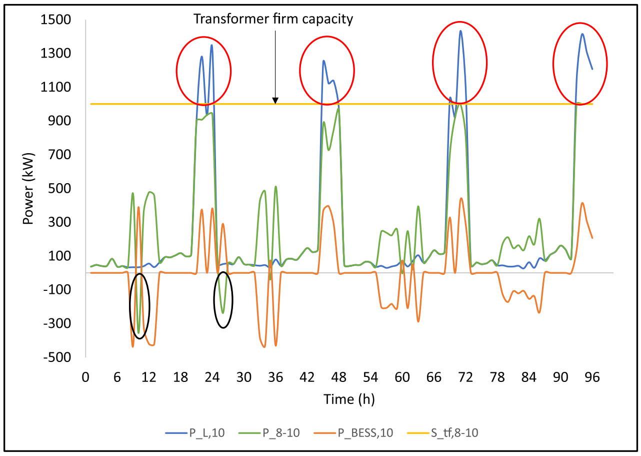

FIGURE 7. Battery active power operation at bus 10 for case 120%.

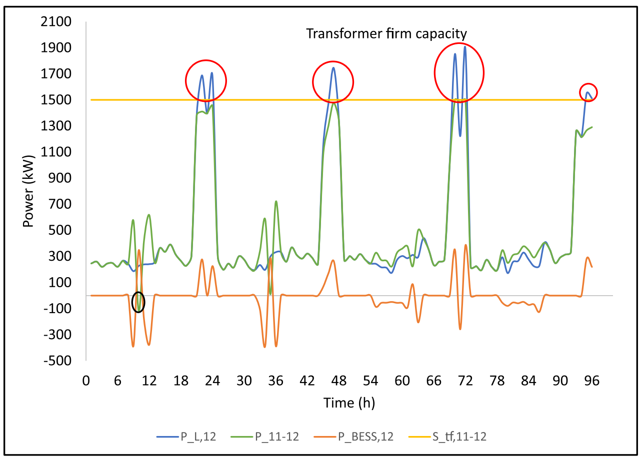

FIGURE 8. Battery active power operation at bus 12 for case 120%.

The figures 11 to 15 below show the operation of the reactive power for the same BESSs.

These figures demonstrated the provision of reactive power from the BESS to the system. In multiple instances, there was a reverse reactive power flow (marked by black) in the feeder, which signifies the reactive power compensation from the BESS to its connected and other loads.

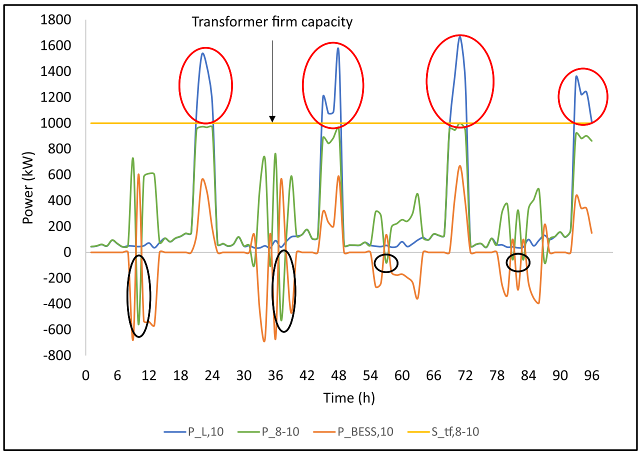

FIGURE 9. Battery active power operation at bus 10 for case 140%.

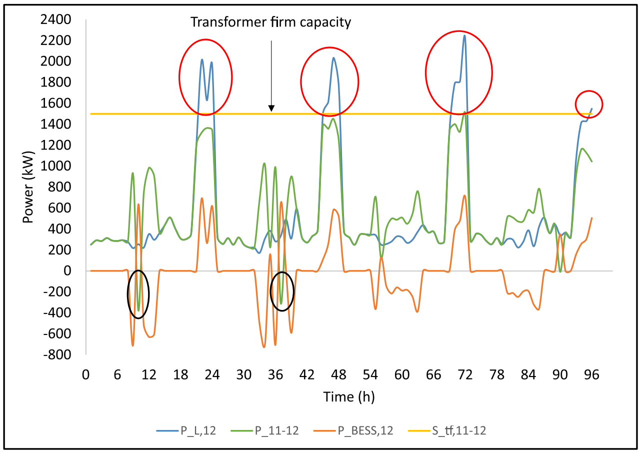

FIGURE 10. Battery active power operation at bus 12 for case 140%.

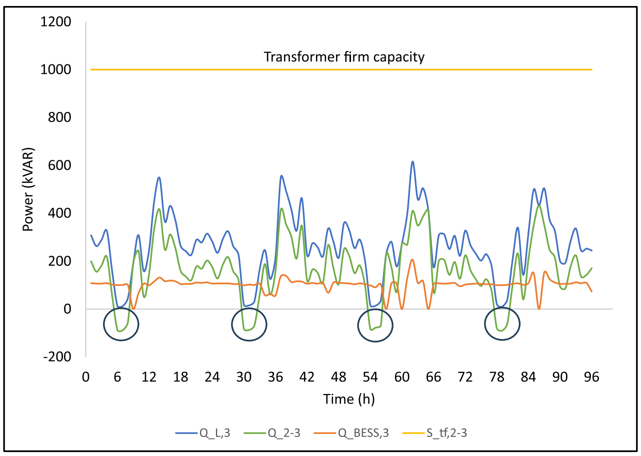

FIGURE 11. Battery reactive power operation at bus 3 for case 120%.

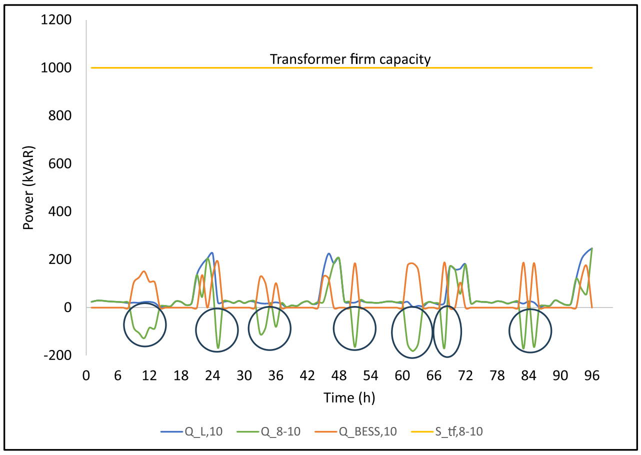

FIGURE 12. Battery reactive power operation at bus 10 for case 120%.

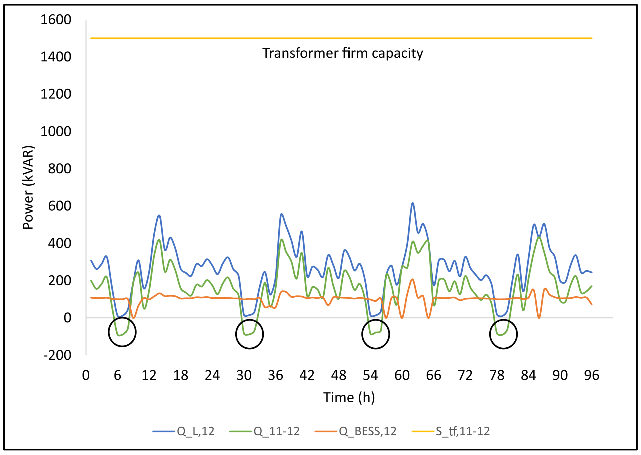

FIGURE 13. Battery reactive power operation at bus 12 for case 120%.

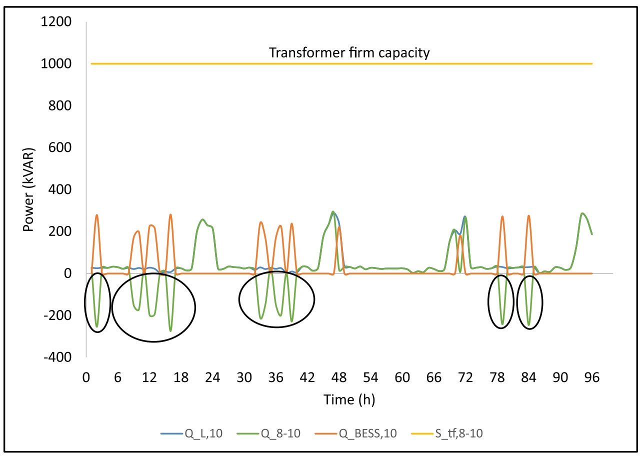

FIGURE 14. Battery reactive power operation at bus 10 for case 140%.

Figure 16 shows the PV capacity penetration in the system, with a clear trend of penetration increase as demand increases. As for Figure 17, the PV power output is shown subjected to variability. To validate the results, we ran the optimization model without having BESS and PV as decision variables, and the results prove that including BESS and PV as potential upgrade elements do indeed provide a lower-cost solution, as seen in Table 5.

Figures 18, 19, and 20 demonstrate the voltage fluctuations for the studied cases. It shows that the voltage magnitude was maintained within the acceptable range (0.9-1.1 pu) at all buses for all time instances considered.

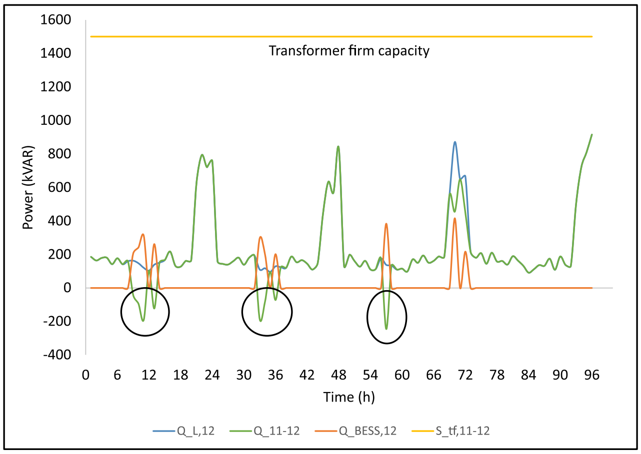

FIGURE 15. Battery reactive power operation at bus 12 for case 140%.

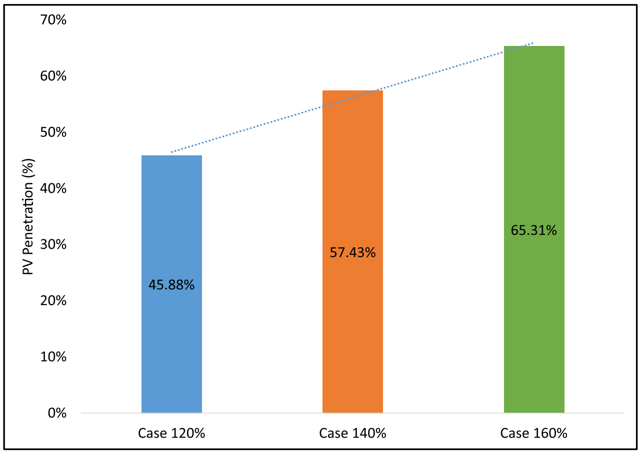

FIGURE 16. PV penetration for all cases.

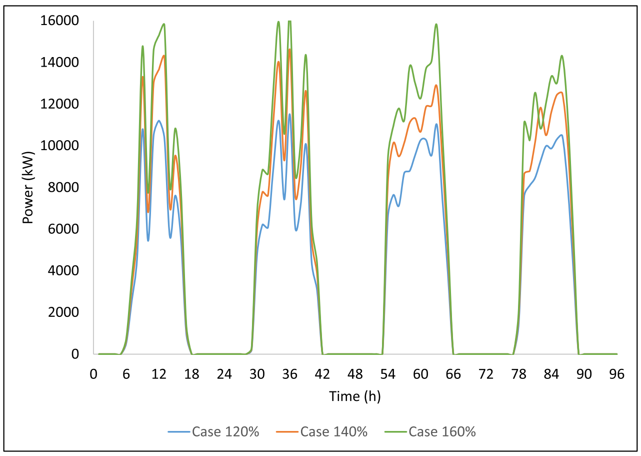

FIGURE 17. PV power output for all cases.

2) CASE B: DISTRIBUTION FEEDER DESIGN

In this simulation study, it is assumed that a distribution feeder will be designed which has a similar topology to Figure 1 to investigate the possibility of incorporating PVs and BESSs in the distribution network. The decision variables include the capacities of the PVs, BESSs, transformers, and cables for a scaled demand of 100%, 120%, 140%, and 160%.

TABLE 5. Cost comparison for test case A.

Scaled demand	120%	140%	160%
Total Cost (Millions)	121.68	142.51	163.26
Total Cost without BESS and PV in the model (Millions)	160.22	187.80	215.03
Δ Cost (Millions)	38.54	45.29	51.77

TABLE 6. Network design for 100% load demand of test case B.

Bus	Electrical Apparatus	Capacity (kVA)
2-3	Transformer	978
2-4	Transformer	879
5-6	Transformer	1104
5-7	Transformer	886
8-9	Transformer	959
8-10	Transformer	701
11-12	Transformer	960
11-13	Transformer	1548
14-15	Transformer	999
14-16	Transformer	1095
14-17	Transformer	1160
14-18	Transformer	957
1-2	Cable	2 (units)
2-5	Cable	1 (unit)
2-8	Cable	1 (unit)
8-11	Cable	1 (unit)
11-14	Cable	1 (unit)
1	PV	14248 (kW)

TABLE 7. Battery energy storage system for 100% load demand of test case B.

Bus	BESS rating	
	Power (kW)	Energy (kWh)
3	105	102
4	280	266
6	56	53
7	145	178
9	83	79
10	406	1158
12	731	1855
13	260	381
15	222	230
16	24	68
17	117	152
18	159	203

For Case B, the assumption is that a new feeder is to be installed, and it is required to determine the needed cables, transformers, BESS, and PVs to supply similar load demands and topology to Case A. The results indicated similar planning features as in Case A, where the BEES is a feasible solution for all studied cases. The design plan and associated cost are shown in Tables 6 to 10. The relatively small difference in total costs between upgrading the feeder (Case A) and designing a new feeder (Case B) for each respected load demand increase, signifies that the original feeder design (Table 1) is unoptimized.

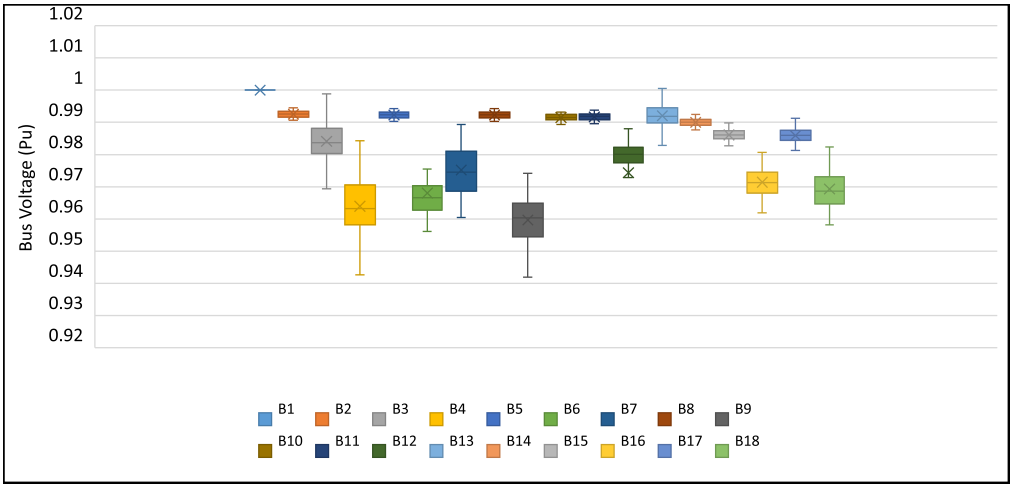

FIGURE 18. Bus voltage fluctuations for the 120% case.

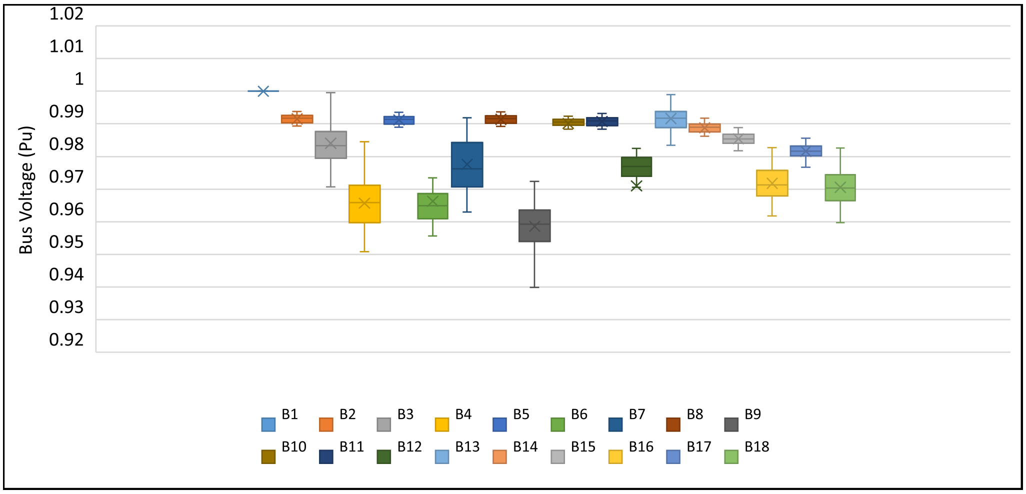

FIGURE 19. Bus voltage fluctuations for the 140% case.

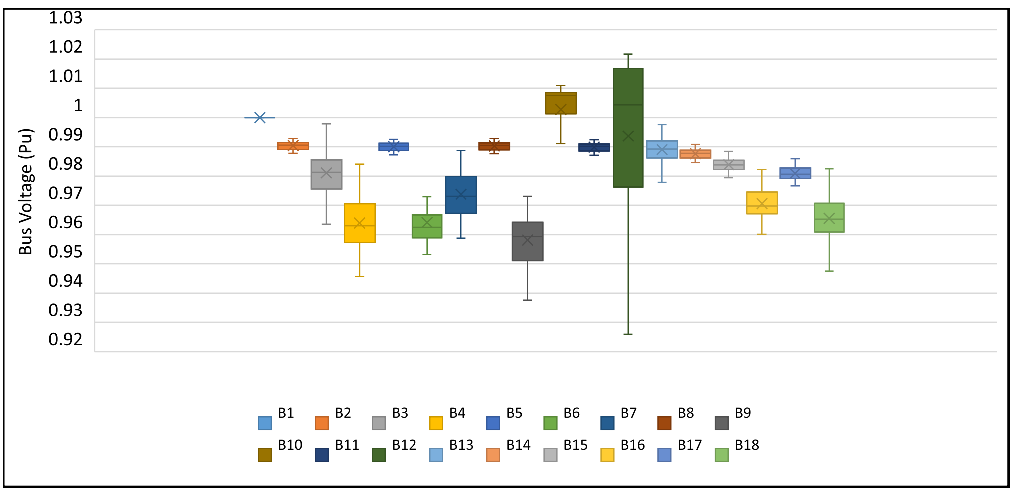

FIGURE 20. Bus voltage fluctuations for the 160% case.

TABLE 8. Network design of test case B.

Bus	Electrical Apparatus	Design Capacity (KVA)		
		120%	140%	160%
2-3	Transformer	981	1370	1358
2-4	Transformer	1060	1268	1337
5-6	Transformer	1306	1470	1750
5-7	Transformer	1089	1232	1466
8-9	Transformer	1076	1303	1476
8-10	Transformer	907	860	975
11-12	Transformer	1109	1243	1645
11-13	Transformer	1900	2192	2514
14-15	Transformer	1204	1338	1532
14-16	Transformer	1312	1430	1697
14-17	Transformer	1351	1749	1944
14-18	Transformer	1052	1222	1395
1-2	Cable	2 (units)	2 (units)	2 (units)
2-5	Cable	1 (unit)	1 (unit)	1 (unit)
2-8	Cable	1 (unit)	2 (units)	2 (units)
8-11	Cable	1 (unit)	1 (unit)	2 (unit)
11-14	Cable	1 (unit)	1 (unit)	1 (unit)
1	PV	16739 (kW)	20217 (kW)	22857 (kW)

TABLE 9. Battery energy storage system for load demand of test case B.

Bus	120%		140%		160%	
	Power (kVA)	Energy (kWh)	Power (kVA)	Energy (kWh)	Power (kVA)	Energy (kWh)
1	-	-	-	-	-	-
2	-	-	-	-	-	-
3	255	243	137	144	375	381
4	316	300	328	346	472	448
5	-	-	-	-	-	-
6	114	108	153	149	95	91
7	106	223	267	297	251	269
8	-	-	-	-	-	-
9	224	213	212	201	327	310
10	524	1494	810	1969	900	2393
11	-	-	-	-	-	-
12	777	1799	961	2374	928	2543
13	258	737	319	501	343	541
14	-	-	-	-	-	-
15	121	115	290	476	287	353
16	30	85	169	360	226	318
17	188	251	-	-	76	80
18	264	527	374	693	410	389

TABLE 10. Total cost of simulated systems for test case B.

Scaled demand	100%	120%	140%	160%
Total Cost (Millions)	107	129	149	170

VI. CONCLUSION

The paper presented an optimization model for the reinforcement plan of a medium voltage distribution feeder. The model considered planning for cables, transformers, BESS, PVs, supplied energy from the grid, and the energy not served, which collectively represents the model's decision variables. The load demand and PV power output uncertainty were considered by incorporating different scenarios and clustering techniques to reduce the computation burden of the model. The BESS operation model was designed to investigate active and reactive power supplies. The model was tested on a local 18-bus distribution feeder in Riyadh, Saudi Arabia. The simulations provided various solutions depending on the demand level. The results showed that the BESS and PV system can be a cost-efficient solution for capacity enhancement or the establishment of new distribution feeders. A continuation of the developed model could involve incorporating electric vehicles (EVs) as a non-stationary energy storage system and other sources of renewable energy.

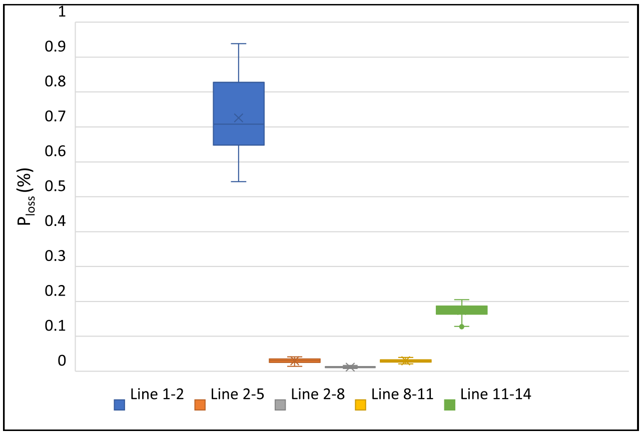

FIGURE 21. Power losses percentage of total power flow.

APPENDIX

This section serves as a justification for omitting the power losses from the developed model. Including the power loss component in the objective function and the constraints would largely impact the performance of the model, which defies the main premise, in providing a fast planning and operation algorithm for distribution feeder reinforcement. Post-simulation current magnitudes $|I_{ij,t}|$ and power loss $P_{loss,ij,t}$ calculations were carried on. The calculations were performed for the case study with the highest demand (case 160%). The results show that the power losses in the network are substantially low ($< 1\%$) compared to the actual power flow in the line, thus an engineering decision was made to omit the power loss component from the model.

$$P_{loss,ij,t} = |I_{ij,t}|^2 r_{ij} \Phi_{c,ij} \tag{45}$$

$$|I_{ij,t}|^2 = \frac{P_{ij,t}^2 + Q_{ij,t}^2}{|V_{i,t}|^2} \tag{46}$$

ACKNOWLEDGMENT

The authors would like to acknowledge the support provided by the Deanship of Research Oversight and Coordination (DROC) at King Fahd University of Petroleum & Minerals (KFUPM) for funding this work through project No. SL222001. The authors would also like to acknowledge the support provided by the Saudi Electricity Company

(SEC), represented by the Research and Development department, for providing valuable data for this project. Power demand data was collected from the monitoring systems related to the Integrated Smart Monitoring and Decision Support System (ISMDSS) project.

REFERENCES

[1] T. A. Short, *Electric Power Distribution Equipment and Systems*. Boca Raton, FL, USA: CRC Press, 2018.

[2] J. D. Glover, M. S. Sarma, and T. Overbye, *Power System Analysis & Design, SI Version*. Boston, MA, USA: Cengage Learning, 2012.

[3] N. Rodrigues, S. Vyas, and A. Datta, ''Two-stage battery energy storage system sizing for distribution transformer overload management,'' in *Proc. Int. Conf. Electr., Electron. Comput. Eng. (UPCON)*, Nov. 2019, pp. 1–6.

[4] S. Zhou, Y. Han, P. Yang, K. Mahmoud, M. Lehtonen, M. M. F. Darwish, and A. S. Zalhaf, ''An optimal network constraint-based joint expansion planning model for modern distribution networks with multi-types intermittent RERs,'' *Renew. Energy*, vol. 194, pp. 137–151, Jul. 2022.

[5] C. K. Das, O. Bass, G. Kothapalli, T. S. Mahmoud, and D. Habibi, ''Overview of energy storage systems in distribution networks: Placement, sizing, operation, and power quality,'' *Renew. Sustain. Energy Rev.*, vol. 91, pp. 1205–1230, Aug. 2018.

[6] V. Vahidinasab, M. Tabarzadi, H. Arasteh, M. I. Alizadeh, M. M. Beigi, H. R. Sheikhzadeh, K. Mehran, and M. S. Sepasian, ''Overview of electric energy distribution networks expansion planning,'' *IEEE Access*, vol. 8, pp. 34750–34769, 2020.

[7] Ž. N. Popovic, V. D. Kerleta, and D. S. Popovic, ''Hybrid simulated annealing and mixed integer linear programming algorithm for optimal planning of radial distribution networks with distributed generation,'' *Electric Power Syst. Res.*, vol. 108, pp. 211–222, Mar. 2014.

[8] T. Zhang, A. E. Emanuel, and J. A. Orr, ''Distribution feeder upgrade deferral through use of energy storage systems,'' in *Proc. IEEE Power Energy Soc. Gen. Meeting (PESGM)*, Jul. 2016, pp. 1–5.

[9] L. Garcia-Garcia, E. A. Paaso, and M. Avendano-Mora, ''Assessment of battery energy storage for distribution capacity upgrade deferral,'' in *Proc. IEEE Power Energy Soc. Innov. Smart Grid Technol. Conf. (ISGT)*, Apr. 2017, pp. 1–5.

[10] S. B. Pienaar, K. Kusakana, and P. T. Manditereza, ''Usage of battery energy storage systems to defer substation upgrades,'' in *Proc. Open Innov. Conf. (OI)*, Oct. 2018, pp. 151–156.

[11] S. R. Deeba, R. Sharma, T. K. Saha, D. Chakraborty, and A. Thomas, ''Evaluation of technical and financial benefits of battery-based energy storage systems in distribution networks,'' *IET Renew. Power Gener.*, vol. 10, no. 8, pp. 1149–1160, Sep. 2016.

[12] P. Komarnicki, P. Lombardi, and Z. Styczynski, *Electric Energy Storage Systems: Flexibility Options for Smart Grids*. Berlin, Germany: Springer, 2017.

[13] D. G. A. Eller, ''Energy storage trends and opportunities in emerging markets,'' Navigant Consulting, Boulder, CO, USA, Tech. Rep. 1, 2017.

[14] S. Ahmadi, V. Vahidinasab, M. S. Ghazizadeh, K. Mehran, D. Giaouris, and P. Taylor, ''Co-optimising distribution network adequacy and security by simultaneous utilisation of network reconfiguration and distributed energy resources,'' *IET Gener., Transmiss. Distribution*, vol. 13, no. 20, pp. 4747–4755, Oct. 2019.

[15] A. Zhou, H. Zhai, M. Yang, and Y. Lin, ''Three-phase unbalanced distribution network dynamic reconfiguration: A distributionally robust approach,'' *IEEE Trans. Smart Grid*, vol. 13, no. 3, pp. 2063–2074, May 2022.

[16] *System Advisor Model*, Nat. Renew. Energy Lab., Golden, CO, USA, 2021.

[17] C. K. Das, O. Bass, G. Kothapalli, T. S. Mahmoud, and D. Habibi, ''Optimal placement of distributed energy storage systems in distribution networks using artificial bee colony algorithm,'' *Appl. Energy*, vol. 232, pp. 212–228, Dec. 2018.

[18] R. C. Dugan, J. A. Taylor, and D. Montenegro, ''Energy storage modeling for distribution planning,'' *IEEE Trans. Ind. Appl.*, vol. 53, no. 2, pp. 954–962, Mar. 2017.

[19] A. A. Almehizia, H. M. K. Al-Masri, and M. Ehsani, ''Integration of renewable energy sources by load shifting and utilizing value storage,'' *IEEE Trans. Smart Grid*, vol. 10, no. 5, pp. 4974–4984, Sep. 2019.

[20] A. Walsh, ''A guide to using total cost of ownership when purchasing distribution transformers,'' UN Environment Programme Global Environmental Facility United for Efficiency (U4E), Paris, France, Tech. Rep. 1, 2022.

[21] C. Coffrin, H. L. Hijazi, and P. Van Hentenryck, ''DistFlow extensions for AC transmission systems,'' 2015, *arXiv:1506.04773*.

[22] S. Lei, J. Wang, C. Chen, and Y. Hou, ''Mobile emergency generator pre-positioning and real-time allocation for resilient response to natural disasters,'' *IEEE Trans. Smart Grid*, vol. 9, no. 3, pp. 2030–2041, May 2018.

[23] T. Ding, Y. Lin, G. Li, and Z. Bie, ''A new model for resilient distribution systems by microgrids formation,'' *IEEE Trans. Power Syst.*, vol. 32, no. 5, pp. 4145–4147, Sep. 2017.

[24] S. Yao, P. Wang, and T. Zhao, ''Transportable energy storage for more resilient distribution systems with multiple microgrids,'' *IEEE Trans. Smart Grid*, vol. 10, no. 3, pp. 3331–3341, May 2019.

[25] X. Chen, W. Wu, and B. Zhang, ''Robust restoration method for active distribution networks,'' *IEEE Trans. Power Syst.*, vol. 31, no. 5, pp. 4005–4015, Sep. 2016.

[26] C. Wang, S. Lei, P. Ju, C. Chen, C. Peng, and Y. Hou, ''MDP-based distribution network reconfiguration with renewable distributed generation: Approximate dynamic programming approach,'' *IEEE Trans. Smart Grid*, vol. 11, no. 4, pp. 3620–3631, Jul. 2020.

[27] S. Xia, K. W. Chan, X. Luo, S. Bu, Z. Ding, and B. Zhou, ''Optimal sizing of energy storage system and its cost-benefit analysis for power grid planning with intermittent wind generation,'' *Renew. Energy*, vol. 122, pp. 472–486, Jul. 2018.

[28] J. H. Yi, R. Cherkaoui, M. Paolone, D. Shchetinin, and K. Knezovic, ''Expansion planning of active distribution networks achieving their dispatchability via energy storage systems,'' *Appl. Energy*, vol. 326, Nov. 2022, Art. no. 119942.

[29] R. Atia and N. Yamada, ''Sizing and analysis of renewable energy and battery systems in residential microgrids,'' *IEEE Trans. Smart Grid*, vol. 7, no. 3, pp. 1204–1213, May 2016.

[30] A. Trivedi, H. C. Aih, and D. Srinivasan, ''A stochastic cost–benefit analysis framework for allocating energy storage system in distribution network for load leveling,'' *Appl. Energy*, vol. 280, Dec. 2020, Art. no. 115944.

[31] K. Mongird, V. Fotedar, V. Viswanathan, V. Koritarov, P. Balducci, B. Hadjerioua, and J. Alam, ''Energy storage technology and cost characterization report,'' U.S. Dept. Energy (DOE), Oak Ridge, TN, USA, Tech. Rep. 1, 2019.

[32] *Annual Technology Baseline: Electricity*, NREL, Golden, CO, USA, 2022.

ABDULLAH A. ALMEHIZIA (Senior Member, IEEE) received the B.Eng. degree in electrical engineering from King Saud University, Riyadh, Saudi Arabia, in 2010, the M.Eng. degree in electrical engineering from the University of Calgary, Calgary, Canada, in 2014, and the Ph.D. degree in electrical engineering from Texas A&M University, College Station, USA, in 2018. He manages the Joint Center for Smart Grids research between KACST and Saudi Electricity Company (SEC). His main work focuses on technology development, localization, and commercialization. His research interests include renewable energy resources, energy storage integration and optimization, power system planning, operation, economics, and policy.

FAHAD S. AL-ISMAIL (Senior Member, IEEE) received the B.Sc. and M.Sc. degrees in electrical engineering from the King Fahd University of Petroleum & Minerals (KFUPM), Dhahran, Saudi Arabia, in 2009 and 2012, respectively, and the Ph.D. degree in electrical engineering from Texas A&M University, College Station, USA, in December 2016. He is currently an Associate Professor with the Department of Electrical Engineering, KFUPM. His research interests include power system planning and reliability, renewable energy integration, and demand-side management modeling with intermittent resources.